

Infinite Sampling: Efficient and Stable Grouped RL Training for Large Language Models

Liangyu Wang
liangyu.wang@kaust.edu.sa
King Abdullah University of Science
and Technology
Saudi Arabia

Tianjin Huang
t.huang2@exeter.ac.uk
University of Exeter
UK

Huanyi Xie
huanyi.xie@kaust.edu.sa
King Abdullah University of Science
and Technology
Saudi Arabia

Mengdi Li
mengdi.li@kaust.edu.sa
King Abdullah University of Science
and Technology
Saudi Arabia

Xinhai Wang
xinhai.wang@kaust.edu.sa
King Abdullah University of Science
and Technology
Saudi Arabia

Di Wang
di.wang@kaust.edu.sa
King Abdullah University of Science
and Technology
Saudi Arabia

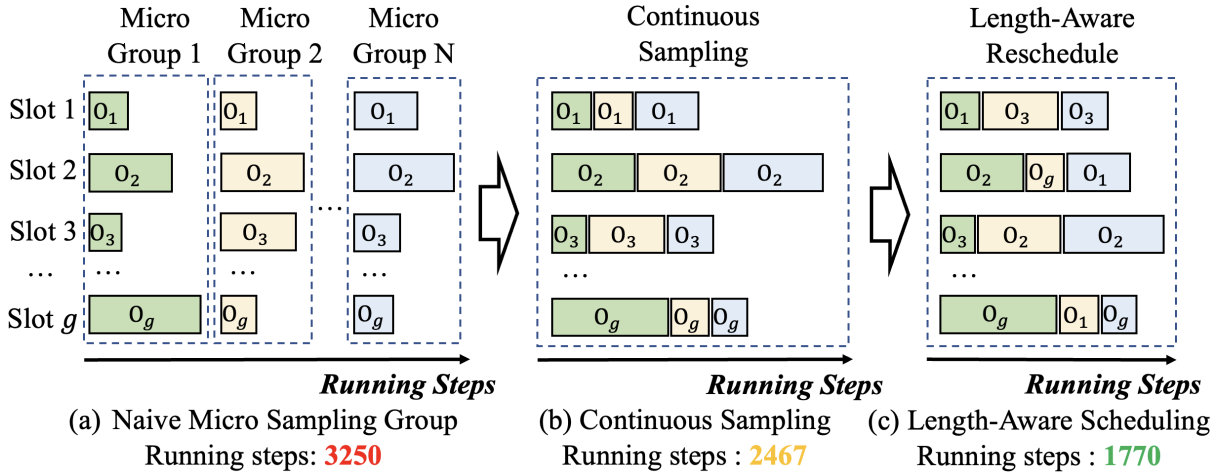


Figure 1: Illustration of the three key components in Infinite Sampling. (a) Naive Micro Sampling Group: Samples are divided into fixed-size micro groups, which are decoded sequentially to reuse shared KV cache but underutilize available compute. (b) Continuous Sampling: Token-level interleaving across micro groups reduces idle time and improves throughput. (c) Length-Aware Scheduling: A predictive scheduler estimates prefix-conditioned sequence lengths and reorders decoding, further optimizing throughput.

Abstract

Group-based reinforcement learning algorithms such as Group Reward Policy Optimization (GRPO) have proven effective for fine-tuning large language models (LLMs) with human feedback. However, generating and storing multiple responses per prompt incurs substantial memory overhead, especially as the sample group size increases, limiting scalability under constrained hardware.

We propose **Infinite Sampling**, a framework that enables efficient and stable GRPO training by decoupling group size from GPU memory usage. It consists of: (1) *micro sampling groups* that decompose large groups into memory-feasible rounds; (2) *continuous sampling* that interleaves generation across groups to improve utilization; and (3) a *length-aware scheduler* combining token-conditioned sequence length prediction with a two-stage plan: global grouping via FPTAS and runtime refill via SJF.

Experiments show that our Micro Sampling Groups reduce peak memory usage by over 50% compared to full-group decoding (e.g.,

from 21.55 GB to 10.64 GB on Qwen3-1.7B). Building on this, Infinite Sampling improves throughput by over 25% compared to the naive micro sampling group method, reducing decoding steps while maintaining full-length completions and memory usage. Our hybrid scheduling ensures efficient and stable GRPO training with larger groups under realistic GPU memory constraints.

1 Introduction

Large language models (LLMs), like GPT [1, 19], Llama [9, 28, 29], or DeepSeek [6], fine-tuned with reinforcement learning from human feedback (RLHF) have achieved state-of-the-art performance in aligning AI outputs with human intent. A common and effective approach in this setting is *Group Reward Policy Optimization (GRPO)* [25], which generates multiple responses per prompt and uses their aggregated rewards to stabilize policy updates. Earlier RLHF pipelines, such as InstructGPT [16], relied on Proximal Policy

Optimization (PPO) [24], but methods like GRPO simplify optimization by using reward baselines across sampled groups and eliminating the need for critic networks.

However, scaling the group size G — the number of sampled completions per prompt — is memory-intensive, especially during autoregressive decoding where each output requires maintaining a separate KV cache. This memory bottleneck often prevents practitioners from utilizing large group sizes, thereby limiting the effectiveness of GRPO.

To overcome this limitation, we propose **Infinite Sampling**, a novel framework for enabling large-group GRPO training under constrained memory. Our approach builds upon the idea of *micro sampling groups*, where the full group of size G is decomposed into smaller subgroups decoded sequentially. While this technique allows KV cache reuse across micro groups and reduces peak memory usage, it introduces idle GPU periods — or *bubbles* — between consecutive decoding stages, harming throughput.

To mitigate these inefficiencies, we introduce *continuous sampling*, a new decoding paradigm inspired by *continuous batching* in LLM inference systems such as vLLM [12] and SGLang [33]. Unlike continuous batching, which dynamically combines multiple unrelated user requests [34], continuous sampling stitches together *outputs from the same prompt* across micro groups using a shared prefill KV cache. This enables *interleaved decoding* of multiple micro groups, significantly reducing idle time and improving GPU utilization.

However, naively interleaving micro groups can trigger memory spikes when multiple long sequences are decoded concurrently. To mitigate this, we propose a two-stage length-aware scheduling strategy. First, we estimate sequence lengths by sampling a short prefix of each completion and conditioning prediction on these early tokens. This token-conditioned estimation—akin to speculative decoding [18]—yields significantly reliable length signals. Next, we combine this with a hybrid scheduling algorithm: a global grouping phase based on a *fixed-point approximation scheme* (FP-TAS), followed by a slot-level *shortest-job-first* (SJF) refill policy during decoding. This design dynamically prioritizes short sequences, achieving a favorable balance between throughput and memory stability.

Contributions. Our contributions are summarized as follows:

- We propose **Infinite Sampling**, a general framework for efficient GRPO training under memory constraints. It decouples sample group size from GPU memory usage by introducing two techniques: (1) *micro sampling groups*, which decompose large groups into memory-feasible decoding rounds, and (2) *continuous sampling*, which interleaves generation across micro groups using a shared prompt cache.
- We design a **length-aware decoding scheduler** to address runtime inefficiencies introduced by micro sampling. It combines prefix-based length prediction with a two-stage scheduling strategy: a global fixed-point approximation (FP-TAS) for balanced group formation, and a slot-level shortest-job-first (SJF) refill policy for dynamic slot reuse.
- We implement and evaluate Infinite Sampling on GRPO training with state-of-the-art LLMs (Qwen3 1.7B/8B). Our *Infinite Sampling* reduce peak memory usage by over **50%**

compared to full-group decoding (e.g., from 21.55 GB to 10.64 GB on Qwen3-1.7B with group size 32), enabling training with large groups under tight memory budgets. On top of this, *naive micro sampling* improves decoding throughput by avoiding full-group parallelism, while *continuous sampling* further reduces decoding steps by mitigating idle time. Finally, our full Infinite Sampling framework—with slot-level scheduling—achieves up to **45%** reduction in decoding steps (e.g., 3250 to 1770 on GSM8K), while preserving full-length completions to ensure stable GRPO training.

2 Preliminary

2.1 Large Language Models (LLMs) Decoding via KV Cache

Autoregressive language models decode text token-by-token by attending to previously generated tokens. To avoid recomputing attention over the entire prefix at each step, modern LLMs cache key and value (KV) tensors from past layers during decoding. This mechanism, known as the KV cache [17, 27], significantly accelerates inference by reusing previously computed attention states.

During decoding, each new token requires a forward pass through all transformer layers, where the current token attends to both cached and current representations. As a result, the KV cache grows linearly with the sequence length and model depth. In typical LLM implementations, each response maintains a dedicated KV buffer across all decoder layers and heads.

While KV caching improves efficiency, it introduces substantial memory overhead when decoding multiple sequences concurrently. In GRPO-style training, where G completions are generated per prompt, the total memory footprint scales linearly with G , sequence length, and model size. This makes KV cache the primary memory bottleneck when training with large sample groups.

2.2 Group Relative Policy Optimization (GRPO) for LLMs

Group Reward Policy Optimization (GRPO) [25] is an enhanced variant of the widely used policy gradient reinforcement learning algorithm, Proxy Policy Gradient (PPO) [24], which is specially designed to improve memory and computation efficiency. PPO relies on a value model to predict the state value of a generated response for advantage calculation [23], where the value model is often initialized with a pretrained LLM of comparable size to the policy model and jointly trained in using supervised learning. Instead, GRPO eliminates the need for a value model by estimating advantages using a Monte Carlo method. It calculates advantages based on the rewards of a group of randomly sampled outputs, significantly reducing memory and computational overhead while ensuring effective policy optimization.

Specifically, GRPO generates a group of outputs for a given prompt x by randomly sampling from the policy π_θ :

$$\{O_1, O_2, \dots, O_G\} \sim \pi_\theta(\cdot | x), \quad (1)$$

where, G is a hyperparameter that determines the group size, i.e., the number of outputs sampled for each prompt x . The advantages

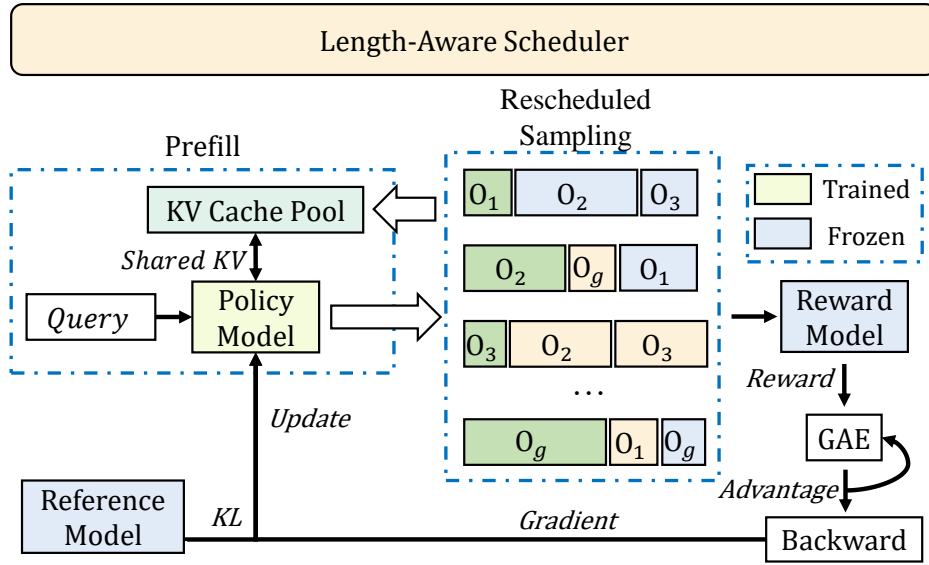


Figure 2: Overview of Infinite Sampling. Given a query, all completions share a prefilled KV cache. (1) *Micro Sampling Groups* (colored) partition large groups into memory-feasible rounds. (2) *Continuous Sampling* interleaves token-level decoding to maximize slot utilization. (3) *Length-Aware Scheduling* predicts prefix-conditioned lengths and orchestrates decoding via global grouping (FPTAS) and slot-level SJF refill. Generated sequences are scored and updated through standard GRPO training.

are estimated using the normalized rewards within the group as:

$$A_i = \frac{r_i - \bar{\mathbf{r}}}{\sigma(\mathbf{r})}, i \in \{1, 2, \dots, G\}, \quad (2)$$

where $\mathbf{r} = \{r_1, r_2, \dots, r_G\}$ represents the rewards corresponding to the group of sampled outputs. These rewards can be derived either from a rule-based reward function or a learned reward model. $\bar{\mathbf{r}}$ and $\sigma(\mathbf{r})$ denote the mean and standard deviation of the rewards in the group, respectively. Based on the estimated advantages, the policy model in GRPO is optimized similarly to PPO, using the following optimization objective

$$\mathcal{J}_{\text{GRPO}}(\theta) = \frac{1}{G} \sum_{i=1}^G \frac{1}{|O_i|} \sum_{t=1}^{|O_i|} \left\{ \min \left[\lambda_t(\theta) A_{i,t}, \text{clip}(\lambda_t(\theta), 1-\epsilon, 1+\epsilon) A_{i,t} \right] - \beta \mathbb{D}_{\text{KL}}[\pi_\theta \parallel \pi_{\text{ref}}] \right\}, \quad (3)$$

where $\lambda_t(\theta) = \frac{\pi_\theta(o_{i,t} | x, O_{i,<t})}{\pi_{\theta_{\text{old}}}(o_{i,t} | x, O_{i,<t})}$ is the ratio of predicted probability of token $o_{i,t}$ under the current policy model θ to that under the old policy model θ_{old} , which was used to sample the output group. $A_{i,t} = A_i$ for $t \in \{1, 2, \dots, |O_i|\}$, where $|O_i|$ is the number of tokens in output O_i . ϵ is a hyperparameter controlling the clipping range for conservative updates, and β is a hyperparameter controlling the weight of the KL-divergence constraint with respect to a reference policy model π_{ref} . For further details on the optimization objective, we recommend referring to the PPO and GRPO paper.

The group size G is a critical hyperparameter that significantly impacts the estimation of advantages, thereby influencing the optimization stability and the performance of the resulting policy model. According to standard Monte Carlo principles [11, 14], increasing

the group size typically improves the accuracy of advantage estimation by incorporating more samples. However, scaling up the group size G introduces substantial overhead. In particular, larger G leads to higher memory consumption during autoregressive decoding, as each sample requires a separate KV cache. These constraints place significant pressure on GPU memory, often making large-group training impractical in real-world settings. To overcome this limitation, we propose *Infinite Sampling*, a framework that decouples the group size G from memory usage by introducing micro-batching, token-level interleaving, and dynamic scheduling strategies.

3 Method

We propose **Infinite Sampling**, a decoding framework that enables large-group GRPO training under tight memory budgets. As illustrated in Figure 2, our framework consists of three components: (1) *Micro Sampling Groups*, which decompose large groups into memory-feasible decoding rounds; (2) *Continuous Sampling*, which streams token-level generation across samples to fully utilize decoding slots; and (3) a *Length-Aware Scheduling* module that predicts token-conditioned sequence lengths and orchestrates both global group planning and reactive runtime scheduling. This design enables high-throughput sampling while maintaining tight control over KV memory footprint and sample-level parallelism.

3.1 Micro Sampling Group: Memory-Efficient Sampling

Generating a large number of samples G per prompt, as required in Group Reward Policy Optimization (GRPO), incurs a prohibitive memory cost. This is because autoregressive decoding allocates a separate key-value (KV) cache buffer for each sampled sequence,

and the memory footprint scales linearly with G . Directly decoding all G sequences in parallel quickly exceeds the available GPU memory, particularly for long sequences and large models.

To address this challenge, we propose to decompose the full sample group into N smaller *micro sampling groups*, each of size $g = G/N$. Instead of allocating memory for all G samples at once, we decode only one micro group at a time and reuse a shared memory region for the KV cache across groups. This approach caps the peak decoding memory at the cost of a single micro group, enabling us to support larger effective group sizes without exceeding hardware limits.

KV Cache Pooling. We maintain a fixed-size memory pool capable of storing the KV cache for up to g active sequences. This pool is initialized before sampling begins and reused across all micro groups. During the decoding of a micro group, its KV cache is dynamically written into this pool. Once decoding finishes for the current group, its cache is cleared and the memory is reassigned back to the pool. Importantly, we retain the prefill KV cache for the prompt itself, which is shared by all groups. This allows us to avoid recomputing the prompt context and only manage memory for the response portion of each group.

Figure 1(a) illustrates this process. At each stage, the memory allocated for one micro group is overwritten by the next, enabling bounded-memory decoding. This scheme offers a simple yet effective trade-off: although we introduce some sequential processing (one group at a time), we gain the ability to scale to arbitrarily large group sizes within fixed memory.

3.2 Continuous Sampling: Interleaved Generation Strategies

While micro sampling enables memory-efficient decoding, it introduces a fundamental throughput bottleneck due to its sequential execution pattern. Specifically, in the standard micro sampling design, the group of G samples is partitioned into N micro groups of size $g = G/N$, and each group is decoded one after another to stay within the memory budget. Although samples within a micro group are decoded in parallel, *inter-group barriers* introduce idle GPU slots when short sequences finish early and must wait for longer ones to complete before proceeding to the next group. This leads to underutilization of available compute, especially under high sample-length variance.

To address this, we introduce **continuous sampling**, a decoding paradigm that interleaves token generation across samples to maintain high utilization of decoding slots while preserving the memory efficiency of micro sampling. This strategy is enabled by the fact that all completions in GRPO originate from the same prompt and hence share the same prefill context. Figure 1(b) illustrates the token-level interleaving enabled by continuous sampling.

Two Modes of Continuous Sampling. Our Continuous sampling can be implemented in two distinct modes, each with its own trade-offs:

(1) *Fixed-Slot Continuous Sampling (Figure 3(a)).* In this mode, the total group of size G is still divided into N micro groups, each of fixed size $g = G/N$. Over the N micro-group rounds, each decoding slot outputs one sequence per round, thus N sequences in total. As soon as any sequence in the group completes, a new sequence is

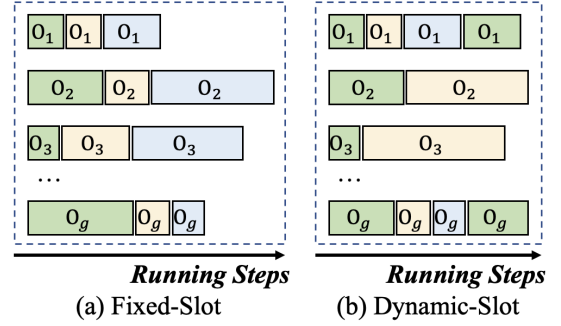


Figure 3: Two Modes of Continuous Sampling. (a) In Fixed-Slot mode, exactly N sequences will be generated for each row, maintaining consistent slot utilization but potentially suffering from idle slots due to length variance. (b) In Dynamic-Slot mode, slots are immediately reused as soon as a sequence finishes, maximizing utilization but sacrificing group structure.

launched in its place, forming the next micro group in the following decoding step. This design maintains a uniform group size at each stage, facilitating micro-batched reward computation and consistent slot usage. Importantly, micro groups may overlap in time—there is no need to wait for the entire group to finish before starting the next. This design enables structured yet flexible decoding aligned with group-based training pipelines.

(2) *Dynamic-Slot Continuous Sampling (Figure 3(b)).* In contrast, this mode does not enforce uniform micro group sizes. Instead, decoding proceeds in a fully streaming fashion: as soon as a sequence completes, its slot is immediately reassigned to a new sample, regardless of how many are currently active. The only constraint is that a total of G sequences must be generated in the end. This strategy maximizes slot throughput but sacrifices structural regularity, making it less compatible with micro-batched updates. Moreover, dynamic-slot scheduling may introduce length bias, where shorter sequences are favored due to faster turnover.

Discussion and Implications. Our system supports both fixed-slot and dynamic-slot continuous sampling. The fixed-slot variant provides consistent micro-batched structure and fairness, but may suffer from idle compute when short sequences must wait for longer ones in the same group. The dynamic-slot variant improves responsiveness and throughput by fully interleaving decoding, yet introduces potential bias favoring shorter sequences. To alleviate the efficiency bottlenecks in fixed-slot sampling, we introduce a *length-aware scheduling strategy* in Section 3.3. By estimating sequence lengths ahead of time and balancing group assignments accordingly, this scheduler smooths per-slot decoding time and maximizes utilization under the fixed-slot setting.

Shared Prompt KV and Sample-Level Cache Lifecycle. As in Section 3.1, all completions share the same prompt KV cache computed during the prefill phase. Each active sample maintains a separate KV buffer for its response tokens, which is recycled upon completion to support new samples within bounded memory.

Comparison with Continuous Batching. At first glance, our continuous sampling method (Figure 6b) may appear similar to

continuous batching techniques (Figure 7) developed for LLM inference systems, such as vLLM and SGLang. However, the two differ in both purpose and implementation. Continuous batching targets *multi-user inference* workloads where each request originates from a distinct prompt. These systems merge unrelated prompts and decode them in shared compute steps, relying on asynchronous request arrival. In contrast, our setting is tailored for *training-time sampling* in GRPO, where all completions are derived from a single prompt. This enables us to compute the prompt KV cache once and reuse it across all samples—an optimization that is not applicable in inference batching. Furthermore, we maintain full control over the sampling loop and cache lifecycle, allowing for token-aware, per-sample scheduling and cache recycling. These characteristics enable more aggressive memory reuse and scheduling strategies, beyond what continuous batching systems support.

3.3 Length-Aware Scheduling: From Static Group Pre-Planning to Adaptive Runtime Scheduling

While continuous sampling interleaves decoding across micro groups to improve throughput, it introduces a new challenge: simultaneous decoding of multiple long sequences can still lead to memory spikes due to cumulative KV cache usage. Compared to the naive micro group strategy described in Section 3.1, the Fixed-Slot Continuous Sampling mode in Section 3.2 improves GPU utilization by filling all slots continuously. However, it remains limited by the “longest sequence” effect—i.e., shorter sequences must wait for the longest one in the end, constraining overall throughput. To address this, we propose a **two-stage scheduling strategy** that combines *offline prefix-based global planning* with *online memory-aware dynamic scheduling*, explicitly designed to mitigate this bottleneck under the fixed-slot constraint.

Prefix Sampling and Length Estimation. To estimate response lengths before full decoding, we first sample a short prefix (e.g., the first k tokens) for each output and predict its final length using a token-conditioned estimator. In contrast to inference-time length prediction—where prompts vary across samples—our setting generates multiple responses from the same prompt. Therefore, prompt-only predictors fail to distinguish among different completions. To address this, we concatenate the prefix to the original prompt to form a pseudo-prompt, preserving the individuality of each sample. This pseudo-prompt is then passed to the predictor. This design provides lightweight yet informative length signals for scheduling. We defer detailed implementation of the predictor to Section 4.

Stage 1: Static Group Pre-Planning via FPTAS. To construct memory-efficient decoding plans prior to generation, we formulate micro group assignment as a classical multiprocessor scheduling problem: given a set of tasks (samples) with estimated execution costs $\{\hat{l}_1, \dots, \hat{l}_G\}$, we aim to partition them into N bins (micro groups) such that the total cost in each bin remains below a predefined memory threshold, and the overall makespan—i.e., the maximum memory load across groups—is minimized. To this end, we adapt a fixed-point approximation scheme (FPTAS) (Algorithm 2) for bin packing with additive error tolerance ϵ . This produces a near-optimal grouping plan that balances memory usage across groups

Algorithm 1 Two-Stage Length-Aware Scheduling for Fixed-Slot Sampling

Require: Estimated lengths $\{\hat{l}_1, \dots, \hat{l}_G\}$, number of slots g

Ensure: Decoding execution plan under fixed-slot sampling with g active slots

```

1: Phase 1: Static Micro Group Assignment
2: Apply FPTAS-Based Group Assignment (Algorithm 2);
   mask[i] ← (n, j)

3: Phase 2: Runtime Decoding with SJF Refill
4: Initialize active slots  $\mathcal{S} \leftarrow$  first  $g$  samples from mask
5: while not all samples are completed do
6:   for each active slot  $s \in \mathcal{S}$  in parallel do
7:     Decode one token for current sample
8:     if sample in slot  $s$  finishes then
9:       Mark sample as completed and release  $s$ 
10:      Apply Slot-Level SJF Refill (Algorithm 3) to select
        next sample for  $s$ 
11:     end if
12:   end for
13: end while

```

while respecting system constraints. Unlike heuristic clustering (e.g., greedy or round-robin), FPTAS ensures formal guarantees on group balance and minimizes the risk of decoding bottlenecks due to misaligned group assignments. This stage produces a static execution plan that guides the initial sampling order and provides a strong baseline for memory-bounded decoding.

Algorithm 2 FPTAS-Based Micro Group Assignment

Require: Estimated lengths $\{\hat{l}_1, \dots, \hat{l}_G\}$, number of groups N , tolerance ϵ

Ensure: Mapping mask[i] ← (n, j) assigning sample i to group n at position j

```

1:  $S \leftarrow \sum_{i=1}^G \hat{l}_i$ ,  $K \leftarrow \epsilon \cdot S/N$ 
2: for  $i = 1$  to  $G$  do
3:    $\tilde{l}_i \leftarrow \lceil \hat{l}_i/K \rceil$ 
4: end for
5:  $\tilde{C} \leftarrow \lceil \sum_{i=1}^G \tilde{l}_i/N \rceil$ 
6: Initialize  $L_n \leftarrow 0$  (total load of group  $n$ ),  $\mathcal{G}_n \leftarrow \emptyset$  for  $n = 1$  to  $N$ 
7: for each sample  $i$  sorted by descending  $\tilde{l}_i$  do
8:   for  $n = 1$  to  $N$  do
9:     if  $L_n + \tilde{l}_i \leq \tilde{C}$  then
10:      Assign  $i$  to  $\mathcal{G}_n$  with position  $j \leftarrow |\mathcal{G}_n|$ 
11:      Set mask[i] ← (n, j)
12:      Update  $L_n \leftarrow L_n + \tilde{l}_i$ 
13:     break
14:   end if
15: end for
16: end for

```

Stage 2: Runtime Adjustment via Shortest-Job-First (SJF).

While the FPTAS provides a globally optimized plan, static scheduling cannot account for runtime variability such as early termination or mispredicted sequence lengths. To handle these dynamics, we introduce a slot-level online adjustment mechanism based on a shortest-job-first (SJF) (Algorithm 3) policy. During continuous sampling, decoding proceeds in an interleaved fashion, and the number of active slots is bounded by available memory. Whenever a sequence completes and releases its KV cache, we immediately dispatch a new sample into the freed slot. The SJF policy ranks all pending samples by their predicted lengths \hat{l}_i , prioritizing shorter samples to maximize slot turnover and reduce memory contention. Importantly, this adjustment is non-blocking and globally aware: samples from future micro groups may be promoted early if they fit the current memory profile. This transforms the decoding process into a fluid, slot-level stream scheduler that adapts to actual completion signals, amortizes memory spikes, and exploits idle compute across groups.

Together, the global planning of FPTAS and the fine-grained responsiveness of SJF yield a decoding pipeline that is both stable and agile—achieving near-optimal memory distribution while remaining robust to length prediction noise and sampling variance.

Algorithm 3 Shortest-Job-First Refill

Require: Finished slot s , estimated lengths $\{\hat{l}_i\}$, finished set \mathcal{F} , mask mask

Ensure: Assign next sample to slot s

- 1: $C \leftarrow \{i \mid i \notin \mathcal{F} \wedge i \notin \text{mask}\}$
- 2: **if** $C = \emptyset$ **then**
- 3: **return** no refill
- 4: **end if**
- 5: Select $j \leftarrow \arg \min_{i \in C} \hat{l}_i$
- 6: Assign j to slot s at next position $\text{pos}[s]$
- 7: Update $\text{mask}[j] \leftarrow (s, \text{pos}[s])$; increment $\text{pos}[s]$

Benefits. This hybrid strategy balances structured planning with runtime flexibility. Prefix-conditioned predictions allow approximate scheduling without requiring deterministic sampling trajectories, while SJF adjustment ensures robustness to length prediction errors. The combination allows us to scale to large group sizes with stable memory usage, fast slot refill, and high throughput.

A schematic overview of our two-stage scheduling results is shown in Figure 1(c). We summarize the complete procedure in Algorithm 1.

3.4 Reward Computation and Micro-Batched Policy Update

While our main focus is on efficient decoding, the subsequent stages—reward computation, advantage normalization, and policy gradient updates—must also be adapted to the micro sampling setup. Both the reward aggregation and the backward pass are executed in micro batches aligned with the decoding schedule. This ensures consistent memory usage throughout the full GRPO pipeline (Figure 2).

However, the decoding stage remains the dominant cost, especially when generating long sequences. As a result, our method

section emphasizes decoding-side optimizations. For completeness, we describe the reward and training stages in detail.

After decoding, each sampled sequence O_i is scored with a scalar reward r_i , computed as a combination of a reward model score and a KL penalty relative to a reference policy $\pi_{\theta_{\text{ref}}}$:

$$r_i = \text{RM}(O_i, x) - \beta \cdot \log \frac{\pi_{\theta}(O_i \mid x)}{\pi_{\theta_{\text{ref}}}(O_i \mid x)}$$

As mentioned before, we decompose the full sample group of size G into N micro groups:

$$G = N \cdot g, \quad \text{where } g \text{ is the micro group size.}$$

We compute rewards $\{r_i\}_{i=1}^G$ and corresponding advantages in a streaming fashion, processing each micro group $\mathcal{G}^{(n)} = \{O_{i_n}, \dots, O_{i_n+g-1}\}$ independently.

Group-Normalized Advantage per Micro Batch. Although micro groups are processed sequentially, the GRPO formulation requires group-wide normalization. Therefore, we cache per-sample rewards from each micro group and compute the full-group mean reward after all N micro batches, as done in normal GRPO:

$$A_i = r_i - \frac{1}{G} \sum_{j=1}^G r_j.$$

This ensures that gradient updates still reflect the entire sample group distribution.

Micro-Batched Backpropagation. After computing A_i for all $i \in [1, G]$, we launch backpropagation in micro batches. For each micro group $\mathcal{G}^{(n)}$, we compute the token-level GRPO loss:

$$\mathcal{J}_{\text{GRPO}}^{(n)}(\theta) = \frac{1}{g} \sum_{O_i \in \mathcal{G}^{(n)}} \frac{1}{|O_i|} \sum_{t=1}^{|O_i|} \left\{ \min \left[\lambda_t(\theta) A_{i,t}, \text{clip}(\lambda_t(\theta), 1-\epsilon, 1+\epsilon) A_{i,t} \right] - \beta \cdot \mathbb{D}_{\text{KL}}[\pi_{\theta} \parallel \pi_{\theta_{\text{ref}}}] \right\}, \quad (4)$$

where $\lambda_t(\theta) = \frac{\pi_{\theta}(o_{i,t} \mid x, o_{i,<t})}{\pi_{\theta_{\text{old}}}(o_{i,t} \mid x, o_{i,<t})}$ is the token-level importance weight.

Backpropagation is performed incrementally on each $\mathcal{J}_{\text{GRPO}}^{(n)}(\theta)$, enabling memory-efficient training with arbitrarily large group size G .

The total loss can be calculated across all micro groups:

$$\mathcal{J}_{\text{GRPO}}(\theta) = \frac{1}{N} \sum_{n=1}^N \mathcal{J}_{\text{GRPO}}^{(n)}(\theta).$$

Memory Efficiency. This micro-batched pipeline ensures that neither decoding, reward computation, nor backpropagation requires instantiating all G completions in memory simultaneously. It complements Infinite Sampling’s decoding design and enables end-to-end GRPO training with large group sizes under tight memory budgets.

4 Sampling Length Prediction

4.1 Motivation and Difference from Prior Work

Existing work on sequence length prediction (e.g., [2, 10, 18]) primarily focuses on inference settings, where the output length is predicted from the input prompt. These methods assume a one-to-one mapping between prompt and output, which does not hold

in our training scenario. In Group Reward Policy Optimization (GRPO), all samples within a group share the same prompt, and the variation arises only from the stochastic sampling process.

As a result, prompt-only predictors fail to distinguish among different completions. To address this, we introduce a token-conditioned estimation strategy that accounts for each sample’s early generation trajectory.

4.2 Token-Conditioned Prediction via Pseudo-Prompts

To obtain per-sample predictions, we first decode a short prefix of k tokens from the current policy for each sample. These tokens are then concatenated to the original prompt, forming a pseudo-prompt:

$$\hat{l}_i = f_{\text{reg}}(\text{BERT}([x; O_{1:k}]))$$

where x is the original prompt, and $O_{1:k}$ denotes the first k tokens decoded from the policy for sample i . The pseudo-prompt is passed to a pretrained BERT encoder, and the [CLS] token embedding is projected by a regression head to estimate the expected length \hat{l}_i .

We fine-tune a length prediction model using the LMSYS-Chat dataset [32], and adopt a standard BERT encoder architecture [7] for token-conditioned pseudo-prompts regression. During decoding, the BERT model is used in frozen inference mode to estimate lengths with negligible runtime overhead. This setup yields accurate and efficient scheduling signals in practice.

Prefix Reuse Optimization. Since the first k tokens have already been decoded during length estimation, we reuse them during actual decoding to avoid redundant computation. For each sample, decoding resumes from token $k+1$, with its KV cache initialized from the prefix. This design eliminates wasted computation and ensures consistency between estimation and execution.

5 Experiments

5.1 Experimental Setup

We evaluate Infinite Sampling on three tasks: **GSM8K** [3], **MATH** [13], and **KK** [30]. All experiments are run on NVIDIA A100-80GB GPUs using **Qwen3** [31] models of size 1.7B and 8B.

Unless otherwise noted, we set prompt batch size $B = 1$, group Size $G = 32$, Micro Group Size $g = 4$, maximum generation length to 1024 tokens, and generation temperature is 0.8. All reported metrics are averaged over all prompts from all datasets. *Memory* refers to the peak GPU memory usage during decoding (lower is better), and *Running Steps* denotes the total number of decoding steps required to complete all sequences (lower indicates faster decoding). Each running step corresponds to one token-generation round across all g active decoding slots—that is, g tokens are generated in parallel in each step. Therefore, the total number of running steps reflects how efficiently the decoding slots are utilized. Fewer steps indicate better throughput under fixed memory and compute budgets.

5.2 Main Results

Our primary goal is to reduce memory overhead in group-based reinforcement learning by decomposing large sampling groups into memory-efficient micro groups. We compare the peak GPU memory usage of Infinite Sampling under different micro group

sizes ($g = 1, 2, 4$) against a baseline that decodes all $G = 8, 16, 32$ samples in parallel.

Figure 4 reports results on Qwen3-1.7B and Qwen3-8B. Across all configurations, Infinite Sampling consistently reduces memory consumption, with smaller micro groups yielding greater savings. For example, on Qwen3-1.7B with $G = 32$, the baseline requires 21.55 GB of memory, while Infinite Sampling with $g = 1$ reduces this to 10.64 GB, a 51% reduction.

Importantly, baseline memory usage grows nearly linearly with the group size G , reflecting the additive cost of KV caches per sample. In contrast, Infinite Sampling maintains almost constant memory usage across different G , as decoding is bounded by the fixed micro group size g .

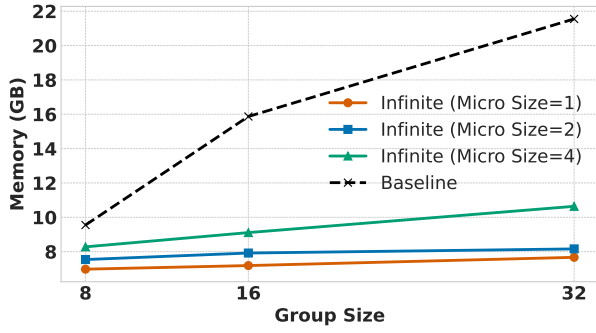
These results confirm that micro sampling enables scaling to large group sizes without exceeding hardware memory limits.

5.3 Ablation Study

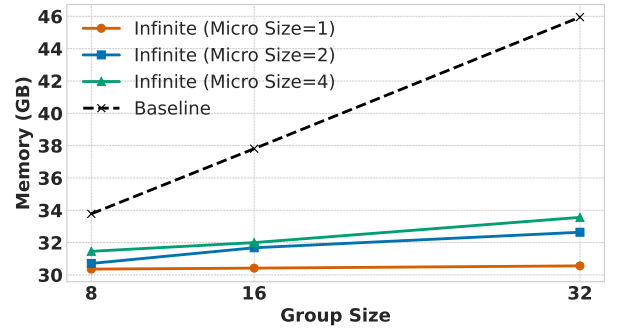
We compare four decoding strategies introduced in Section 3: **Naive Micro Group** (Section 3.1), **Fixed-slot** (Section 3.2), **Dynamic-slot** (Section 3.2), and **Infinite-sampling** (Section 3.3).

Table 1 reports running steps and average sequence length across three datasets and two model sizes. We make the following key observations:

- **Decoding Latency:** Across all tasks, Naive Micro Group consistently results in the highest number of decoding steps. For instance, on the MATH dataset with Qwen3-1.7B, it requires 7005 steps, while Infinite-sampling reduces this to only 5203 steps (a 25.7% improvement). On KK, the reduction is even more pronounced—7037 (Naive) to 5200 (Infinite-sampling), a 26.1% gain.
- **Sequence Length Preservation:** Infinite-sampling and Fixed-slot both preserve the average sequence length, matching that of the Naive Micro Group. For example, on the GSM8K dataset with Qwen3-8B, all three strategies produce an average of 186 tokens, ensuring sample quality is not sacrificed.
- **Dynamic-Slot Tradeoff:** Although Dynamic-slot achieves the fewest decoding steps (e.g., 360 steps on GSM8K with Qwen3-8B), it substantially shortens the generated sequences (e.g., only 21 tokens on average). As discussed in Section 3.2, this is due to length bias introduced by streaming generation and greedy slot reuse, which may negatively impact training stability and reward quality.
- **Offline Scheduling Optimality:** Infinite-sampling * provides a reference lower bound on running steps. For example, on KK with Qwen3-8B, Infinite-sampling * achieves 2586 steps compared to 2599 for the actual Infinite-sampling implementation—demonstrating that the practical scheduling is near-optimal (only 0.5% higher).
- **Stability vs. Efficiency:** Infinite-sampling provides a balanced trade-off, maintaining long outputs while reducing latency. In contrast, Dynamic-slot aggressively optimizes for throughput at the cost of sequence quality, which may be unsuitable for reward-based learning.



(a) Qwen3-1.7B: Infinite Sampling consistently reduces memory usage across micro group sizes.



(b) Qwen3-8B: Even for larger models, Infinite Sampling maintains significant memory savings.

Figure 4: Peak memory usage comparison under different group sizes and micro group configurations for Infinite Sampling. The baseline refers to directly decoding all G sequences in parallel. Infinite Sampling achieves substantial memory savings across models.

Table 1: Ablation Study. Running steps and average sequence length of different proposed components. Note: “Infinite-sampling **” represents a theoretical oracle performance, where all responses are scheduled post hoc after generation, allowing the shortest possible execution steps. This serves as a lower-bound reference rather than a practical decoding strategy. All subsequent tables include this reference for comparison.

| Dataset | Method | Qwen3-1.7B | | Qwen3-8B | |
|---------|---------------------|---------------|-------------|---------------|-------------|
| | | Running Steps | Avg Length | Running Steps | Avg Length |
| GSM8K | Naive Micro Group | 3250 | 186 | 3250 | 186 |
| | Fixed-slot | 2467 (x0.75) | 186 (x1.00) | 2467 (x0.75) | 186 (x1.00) |
| | Dynamic-slot | 748 (x0.23) | 72 (x0.39) | 360 (x0.11) | 21 (x0.11) |
| | Infinite-sampling * | 1739 (x0.53) | 186 (x1.00) | 1739 (x0.53) | 186 (x1.00) |
| | Infinite-sampling | 1770 (x0.54) | 186 (x1.00) | 1769 (x0.54) | 186 (x1.00) |
| MATH | Naive Micro Group | 7005 | 602 | 5051 | 395 |
| | Fixed-slot | 6098 (x0.87) | 602 (x1.00) | 4190 (x0.83) | 395 (x1.00) |
| | Dynamic-slot | 1395 (x0.20) | 143 (x0.23) | 1626 (x0.32) | 172 (x0.43) |
| | Infinite-sampling * | 5126 (x0.73) | 602 (x1.00) | 3492 (x0.69) | 395 (x1.00) |
| | Infinite-sampling | 5203 (x0.74) | 602 (x1.00) | 3533 (x0.70) | 395 (x1.00) |
| KK | Naive Micro Group | 7037 | 591 | 4682 | 282 |
| | Fixed-slot | 6129 (x0.87) | 591 (x1.00) | 3550 (x0.75) | 282 (x1.00) |
| | Dynamic-slot | 1104 (x0.16) | 102 (x0.17) | 696 (x0.15) | 38 (x0.13) |
| | Infinite-sampling * | 5089 (x0.72) | 591 (x1.00) | 2586 (x0.55) | 282 (x1.00) |
| | Infinite-sampling | 5200 (x0.74) | 591 (x1.00) | 2599 (x0.56) | 282 (x1.00) |

These results highlight the trade-offs between decoding efficiency and sequence quality. While Dynamic-slot is fastest, Infinite-sampling offers a better balance between speed and GRPO effectiveness.

5.4 Scheduler Choice

We study the impact of different scheduling components introduced in Section 3.3. Table 2 reports the number of running steps under the Fixed-slot setting, using four variants: **Fixed-slot** (no scheduling), **FPTAS only** (only uses static pre-grouping), **SJF only** (only uses slot-level dynamic refill), and **Infinite** (FPTAS + SJF).

We make the following key observations:

- **Slot-Level Scheduling Dominates:** SJF-only consistently yields the greatest reduction in decoding steps among all individual strategies. For instance, on GSM8K with Qwen3-1.7B, SJF reduces the steps from 2467 (Fixed-slot) to 1775, a 28.1% improvement. Similar trends are observed across other datasets, confirming that online dynamic refill is the key factor in improving efficiency.
- **FPTAS Provides Secondary Gains:** The FPTAS-only strategy offers moderate gains over Fixed-slot (e.g., 2100 vs. 2467 on GSM8K), but consistently underperforms SJF. This aligns with its design: FPTAS statically balances load before decoding, which improves average-case slot utilization but

Table 2: Running steps of different scheduling methods.

| Dataset | Schedule Method | Qwen3-1.7B Running Steps | Qwen3-8B Running Steps |
|---------|-----------------|-----------------------------|---------------------------|
| GSM8K | Fixed-slot | 2467 | 2467 |
| | Infinite * | 1739 (x0.70) | 1739 (x0.70) |
| | FPTAS only | 2100 (x0.85) | 2100 (x0.85) |
| | SJF only | 1775 (x0.72) | 1774 (x0.72) |
| | Infinite | 1770 (x0.72) | 1769 (x0.72) |
| MATH | Fixed-slot | 6098 | 4190 |
| | Infinite * | 5126 (x0.84) | 3492 (x0.83) |
| | FPTAS only | 6021 (x0.98) | 4154 (x0.99) |
| | SJF only | 5380 (x0.88) | 3624 (x0.86) |
| | Infinite | 5203 (x0.85) | 3533 (x0.84) |
| KK | Fixed-slot | 6129 | 3550 |
| | Infinite * | 5089 (x0.83) | 2586 (x0.72) |
| | FPTAS only | 6014 (x0.98) | 3531 (x0.99) |
| | SJF only | 5219 (x0.85) | 2695 (x0.76) |
| | Infinite | 5200 (x0.84) | 2599 (x0.73) |

cannot adapt to runtime variation. These results suggest that FPTAS is useful but insufficient on its own, because, as discussed in Section 3.3, it cannot adapt to runtime variability such as early termination or prediction noise. In contrast, SJF dynamically corrects these deviations during decoding, quickly filling idle slots with short sequences. These results highlight that runtime correction is crucial for achieving high decoding throughput and robust memory usage.

- **Infinite Matches the Lower Bound:** The full Infinite scheduling strategy (FPTAS + SJF) consistently performs within 1% of the oracle Infinite-sampling *, which assumes access to all responses before scheduling. For example, on KK with Qwen3-8B, Infinite achieves 2599 steps, while the oracle baseline reaches 2586. This demonstrates that combining global planning with runtime reactivity nearly closes the gap to optimality.

5.5 Effect of Prefix Length k on Prediction Accuracy

To investigate the impact of prefix length on the accuracy of length prediction (Section 4), we evaluate our BERT-based length predictor under different values of $k \in \{1, 2, 4, 8, 16, 32\}$, where k denotes the number of initial tokens sampled from the policy model before estimation.

Figure 5 reports the prediction error across two model scales: Qwen3-1.7B and Qwen3-8B. We observe that increasing k consistently improves prediction accuracy up to a point, with diminishing returns beyond $k = 16$. Notably, the Qwen3-8B model achieves better accuracy than Qwen3-1.7B at every k , likely due to its more consistent output distributions.

Based on these results, we use $k = 16$ as the default prefix length for length prediction in all Infinite Sampling experiments reported in the main paper.

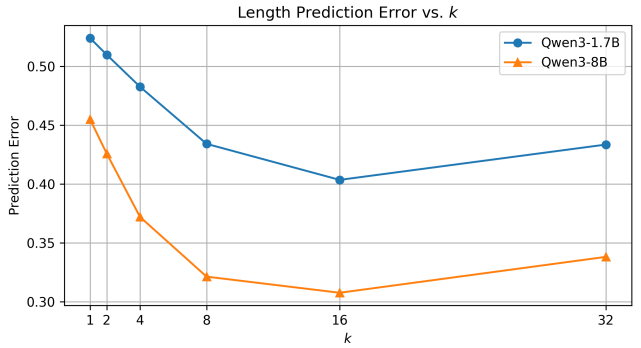


Figure 5: Length prediction error vs. prefix length k . Qwen3-8B consistently achieves lower error, and accuracy improves as more tokens are included for prediction, up to $k = 16$.

6 Related Work

RLHF and Grouped Sampling Optimization. Reinforcement Learning from Human Feedback (RLHF) has become the de facto approach for aligning large language models (LLMs) with human preferences. Early pipelines such as InstructGPT [15] rely on Proximal Policy Optimization (PPO) [24] to fine-tune policies using scalar rewards from a learned reward model. However, PPO introduces complexity due to the use of critic networks and unstable advantage estimation. To mitigate these issues, recent methods such as Direct Preference Optimization (DPO) [20] and Group Reward Policy Optimization (GRPO) propose critic-free, group-normalized objectives. GRPO in particular improves training stability by aggregating scores over multiple sampled completions per prompt. Our work builds directly on group-based reinforcement learning algorithms, such as GRPO, and tackles the underexplored question of how to support large group sizes G under strict memory constraints—a challenge not addressed in prior GRPO literature.

Efficient RLHF Frameworks. Recent RLHF frameworks focus on building general-purpose and efficient infrastructure for running RLHF pipelines. HybridFlow [26] introduces a hybrid programming model that decouples intra-node model computation (using multi-controller execution) and inter-node data orchestration (using a centralized controller), achieving efficient model placement and resharding across training and generation stages. StreamRL [35] and AReal [8] further streamline RLHF actor rollout by improving token-level parallelism and offloading efficiency. In contrast, Infinite-sampling does not propose a general-purpose RLHF framework. Instead, it focuses on decoding efficiency by introducing micro sampling groups and continuous scheduling to maximize GPU utilization and memory throughput during actor rollout. While existing frameworks aim to optimize end-to-end RLHF pipelines through system-level modularity and flexibility, our work complements them by proposing fine-grained decoding strategies that can be integrated into these infrastructures. Our techniques are lightweight and inference-centric, designed to decrease sampling memory usage without requiring changes to reward modeling, training loops, or inter-model protocols.

Batching and KV Cache Optimization. A growing body of work focuses on improving memory efficiency and throughput in

LLM inference through KV cache management and dynamic batching. Notably, vLLM [12] introduces PagedAttention and continuous batching to reuse KV cache and maximize hardware utilization. BatchLLM [34] further enhances cache reuse through prefix-aware batching and reorder-based scheduling. However, these systems are inference-centric and assume independent user requests. Our work adapts these ideas to the training-time setting of RLHF, where all completions originate from the same prompt and must be grouped for reward aggregation. We propose a continuous sampling mechanism tailored for such homogeneous input settings, while also incorporating length-aware scheduling for memory control—something not explored in existing batched decoding systems.

Memory-Efficient LLM Training. Orthogonal to inference efficiency, many efforts have improved memory utilization during training, such as ZeRO [21], ZeRO-Infinity [22], and FlashAttention [4, 5]. These methods target optimizer state sharding, parameter offloading, and fused GPU kernels to reduce memory and bandwidth overheads. Our approach is complementary: rather than optimizing backpropagation or attention itself, we focus on *reducing decoding-time memory* during RLHF training by restructuring how and when sample completions are generated. To our knowledge, we are the first to combine micro sampling, continuous sampling, and slot-level scheduling to support large-group GRPO training under fixed memory budgets.

Summary. In sum, while prior work has studied reward aggregation in RLHF, sequence length prediction for inference, and memory-efficient model execution, none have addressed the unique combination of challenges posed by large-group GRPO training. Our method, **Infinite Sampling**, is the first to jointly address group-level decoding, token-interleaved generation, and adaptive sample scheduling, offering a unified framework for scalable and stable RLHF under memory constraints.

7 Conclusion

We present **Infinite Sampling**, a framework for enabling large-group GRPO training under constrained GPU memory. By decomposing full sample groups into memory-feasible micro groups, interleaving decoding across groups, and applying token-conditioned length-aware scheduling, our method substantially reduces peak memory usage while preserving sample quality. While our approach introduces partial serialization and does not match the theoretical latency of fully parallel decoding, we design continuous sampling and hybrid scheduling (FPTAS + SJF) to mitigate the overhead. This achieves a favorable trade-off between memory efficiency and decoding throughput, enabling stable and scalable GRPO training with large group sizes under realistic hardware constraints. While Infinite Sampling achieves strong memory efficiency and decoding performance, our current implementation assumes all completions originate from a single prompt. Extending our framework to support multi-prompt batches or integrating with more advanced KV cache compression techniques is an interesting direction for future work. We hope this work offers a practical foundation for memory-efficient group-based RLHF optimization at scale.

References

[1] Tom B. Brown, Benjamin Mann, Nick Ryder, Melanie Subbiah, Jared Kaplan, Prafulla Dhariwal, Arvind Neelakantan, Pranav Shyam, Girish Sastry, Amanda

Askeel, Sandhini Agarwal, Ariel Herbert-Voss, Gretchen Krueger, Tom Henighan, Rewon Child, Aditya Ramesh, Daniel M. Ziegler, Jeffrey Wu, Clemens Winter, Christopher Hesse, Mark Chen, Eric Sigler, Matusz Litwin, Scott Gray, Benjamin Chess, Jack Clark, Christopher Berner, Sam McCandlish, Alec Radford, Ilya Sutskever, and Dario Amodei. 2020. Language Models are Few-Shot Learners. arXiv:2005.14165 [cs.CL] <https://arxiv.org/abs/2005.14165>

[2] Seungbeom Choi, Jeongho Goo, Eunjoon Jeon, Mingyu Yang, and Minsung Jang. 2025. ELIS: Efficient LLM Iterative Scheduling System with Response Length Predictor. arXiv:2505.09142 [cs.DC] <https://arxiv.org/abs/2505.09142>

[3] Karl Cobbe, Vineet Kosaraju, Mohammad Bavarian, Mark Chen, Heewoo Jun, Lukasz Kaiser, Matthias Plappert, Jerry Tworek, Jacob Hilton, Reiichiro Nakano, Christopher Hesse, and John Schulman. 2021. Training Verifiers to Solve Math Word Problems. arXiv:2110.14168 [cs.LG] <https://arxiv.org/abs/2110.14168>

[4] Tri Dao. 2023. FlashAttention-2: Faster Attention with Better Parallelism and Work Partitioning. arXiv:2307.08691 [cs.LG] <https://arxiv.org/abs/2307.08691>

[5] Tri Dao, Daniel Y. Fu, Stefano Ermon, Atri Rudra, and Christopher Ré. 2022. FlashAttention: Fast and Memory-Efficient Exact Attention with IO-Awareness. arXiv:2205.14135 [cs.LG] <https://arxiv.org/abs/2205.14135>

[6] DeepSeek-AI, Aixin Liu, Bei Feng, Bing Xue, Bingxuan Wang, Bochao Wu, Chengda Lu, Chenggang Zhao, Chengqi Deng, Chenyu Zhang, Chong Ruan, Damai Dai, Daya Guo, Dejian Yang, Deli Chen, Dongjie Ji, Erhang Li, Fangyun Lin, Fucong Dai, Fuli Luo, Guangbo Hao, Guanting Chen, Guowei Li, H. Zhang, Han Bao, Hanwei Xu, Haocheng Wang, Haowei Zhang, Honghui Ding, Huajian Xin, Huazuo Gao, Hui Li, Hui Qu, J. L. Cai, Jian Liang, Jianzhong Guo, Jiaqi Ni, Jiashi Li, Jiawei Wang, Jin Chen, Jingchang Chen, Jingyang Yuan, Junjie Qiu, Junlong Li, Junxiao Song, Kai Dong, Kai Hu, Kaige Gao, Kang Guan, Kexin Huang, Kuai Yu, Lean Wang, Lecong Zhang, Lei Xu, Leyi Xia, Liang Zhao, Litong Wang, Liyue Zhang, Meng Li, Miaojun Wang, Mingchuan Zhang, Minghua Zhang, Minghui Tang, Mingming Li, Ning Tian, Panpan Huang, Peiyi Wang, Peng Zhang, Qiancheng Wang, Qihao Zhu, Qinyu Chen, Qiusi Du, R. J. Chen, R. L. Jin, Ruiqi Ge, Ruisong Zhang, Ruizhe Pan, Runji Rudra, Runxin Xu, Ruoyu Zhang, Ruyi Chen, S. S. Li, Shanghao Lu, Shangyan Zhou, Shanhuang Chen, Shaoqing Wu, Shengfeng Ye, Shengfeng Ye, Shirong Ma, Shiyu Wang, Shuang Zhou, Shuiping Yu, Shunfeng Zhou, Shuting Pan, T. Wang, Tao Yun, Tian Pei, Tianyu Sun, W. L. Xiao, Wangding Zeng, Wanbiao Zhao, Wei An, Wen Liu, Wenfeng Liang, Wenjun Gao, Wenqin Yu, Wentao Zhang, X. Q. Li, Xiangyu Jin, Xianzu Wang, Xiao Bi, Xiaodong Liu, Xiaohan Wang, Xiaojin Shen, Xiaokang Chen, Xiaokang Zhang, Xiaosha Chen, Xiaotao Nie, Xiaowen Sun, Xiaoxiang Wang, Xin Cheng, Xin Liu, Xin Xie, Xingchao Liu, Xingkai Yu, Xinnan Song, Xinxia Shan, Xinyi Zhou, Xinyu Yang, Xinyuan Li, Xuecheng Su, Xuheng Lin, Y. K. Li, Y. Q. Wang, Y. X. Wei, Y. X. Zhu, Yang Zhang, Yanhong Xu, Yanhong Xu, Yanping Huang, Yao Li, Yao Zhao, Yaofeng Sun, Yaohui Li, Yaohui Wang, Yi Yu, Yi Zheng, Yichao Zhang, Yifan Shi, Yiliang Xiong, Ying He, Ying Tang, Yishi Piao, Yisong Wang, Yixuan Tan, Yiyang Ma, Yiyuan Liu, Yongqiang Guo, Yu Wu, Yuan Ou, Yuchen Zhu, Yudian Wang, Yue Gong, Yuheng Zou, Yujia He, Yukun Zha, Yunfan Xiong, Yunxian Ma, Yuting Yan, Yuxiang Luo, Yuxiang You, Yuxuan Liu, Yuyang Zhou, Z. F. Wu, Z. Z. Ren, Zehui Ren, Zhenliang Sha, Zhe Fu, Zhen Xu, Zhen Huang, Zhen Zhang, Zhen Xie, Zhengchao Liu, Zhengyan Zhang, Zhewen Hao, Zhibin Gou, Zhicheng Ma, Zhigang Yan, Zhihong Shao, Zhipeng Xu, Zhiyu Wu, Zhongyu Zhang, Zhuoshu Li, Zihui Gu, Zijia Zhu, Zijun Liu, Zilin Li, Ziwei Xie, Ziyang Song, Ziyi Gao, and Zizheng Pan. 2025. DeepSeek-V3 Technical Report. arXiv:2412.19437 [cs.CL] <https://arxiv.org/abs/2412.19437>

[7] Jacob Devlin, Ming-Wei Chang, Kenton Lee, and Kristina Toutanova. 2019. BERT: Pre-training of Deep Bidirectional Transformers for Language Understanding. arXiv:1810.04805 [cs.CL] <https://arxiv.org/abs/1810.04805>

[8] Wei Fu, Jiaxuan Gao, Xujie Shen, Chen Zhu, Zhiyu Mei, Chuyi He, Shusheng Xu, Guo Wei, Jun Mei, Jiashu Wang, Tongkai Yang, Binhang Yuan, and Yi Wu. 2025. AReL: A Large-Scale Asynchronous Reinforcement Learning System for Language Reasoning. arXiv:2505.24298 [cs.LG] <https://arxiv.org/abs/2505.24298>

[9] Aaron Grattafiori, Abhimanyu Dubey, Abhinav Jauhri, Abhinav Pandey, Abhishek Kadian, Ahmad Al-Dahle, Aiesha Letman, Akhil Mathur, Alan Schelten, Alex Vaughan, Amy Yang, Angela Fan, Anirudh Goyal, Anthony Hartshorn, Aobo Yang, Archi Mitra, Archie Sravankumar, Artem Korenev, Arthur Hinsvark, Arun Rao, Aston Zhang, Aurelien Rodriguez, Austen Gregerson, Ava Spataru, Baptiste Roziere, Bethany Biron, Binh Tang, Bobbie Chern, Charlotte Caucheteux, Chaya Nayak, Chloe Bi, Chris Marra, Chris McConnell, Christian Keller, Christophe Touret, Chunyang Wu, Corinne Wong, Cristian Canton Ferrer, Cyrus Nikolaidis, Damien Allonsius, Daniel Song, Danielle Pinte, Danny Livshits, Danny Wyatt, David Esiobu, Dhruv Choudhary, Dhruv Mahajan, Diego Garcia-Olano, Diego Perino, Dieuwke Hupkes, Egor Lakomkin, Ehab AlBadawy, Elina Lobanova, Emily Dinan, Eric Michael Smith, Filip Radenovic, Francisco Guzmán, Frank Zhang, Gabriel Synnaeve, Gabrielle Lee, Georgia Lewis Anderson, Govind Thattai, Graeme Nail, Gregoire Mialon, Guan Pang, Guillem Cucurell, Hailey Nguyen, Hannah Korevaar, Hu Xu, Hugo Touvron, Iliyan Zarov, Imanol Arrieta Ibarra, Isabel Kloumann, Ishan Misra, Ivan Evtimov, Jack Zhang, Jade Copet, Jaewon Lee, Jan Geffert, Jana Vranes, Jason Park, Jay Mahadeokar, Jeet Shah, Jelmer van der Linde, Jennifer Billock, Jenny Hong, Jenya Lee, Jeremy Fu, Jianfeng Chi, Jianyu Huang, Jiawen Liu, Jie Wang, Jiecao Yu, Joanna Bitton, Joe Spisak, Jongsoo

- Park, Joseph Rocca, Joshua Johnstun, Joshua Saxe, Junteng Jia, Kalyan Vasuden Alwala, Karthik Prasad, Kartikeya Upasani, Kate Plawiak, Ke Li, Kenneth Heafield, Kevin Stone, Khalid El-Arini, Krithika Iyer, Kshitiz Malik, Kuenley Chiu, Kunal Bhalla, Kushal Lakhotia, Lauren Rantala-Yearly, Laurens van der Maaten, Lawrence Chen, Liang Tan, Liz Jenkins, Louis Martin, Lovish Madaan, Lubo Malo, Lukas Blecher, Lukas Landzaat, Luke de Oliveira, Madeline Muzzi, Mahesh Pasupuleti, Mannat Singh, Manohar Paluri, Marcia Kardas, Maria Tsimpoukelli, Mathew Oldham, Mathieu Rita, Maya Pavlova, Melanie Kambadur, Mike Lewis, Min Si, Mitesh Kumar Singh, Mona Hassan, Naman Goyal, Narjes Torabi, Nikolay Bashlykov, Nikolay Bogoychev, Niladri Chatterji, Ning Zhang, Olivier Duchenne, Onur Celebi, Patrick Alrassy, Pengchuan Zhang, Pengwei Li, Petar Vasic, Peter Weng, Prajwal Bhargava, Pratik Dubal, Praveen Krishnan, Punit Singh Koura, Puxin Xu, Qing He, Qingxiao Dong, Ragavan Srinivasan, Raj Ganapathy, Ramon Calderer, Ricardo Silveira Cabral, Robert Stojnic, Roberta Raileanu, Rohan Maheswari, Rohit Girdhar, Rohit Patel, Romain Sauvestre, Ronnie Polidoro, Roshan Sumbaly, Ross Taylor, Ruan Silva, Rui Hou, Rui Wang, Saghar Hosseini, Sahana Chennabasappa, Sanjay Singh, Sean Bell, Seohyun Sonia Kim, Sergey Edunov, Shao-liang Nie, Sharan Narang, Sharrath Rapparthi, Sheng Shen, Shengye Wan, Shruti Bhosale, Shun Zhang, Shmoran Vandenhende, Soumya Batra, Spencer Whitman, Sten Sootla, Stephane Collet, Suchin Gururangan, Sydney Borodinsky, Tamar Herman, Tara Fowler, Tarek Sheasha, Thomas Georgiou, Thomas Scialom, Tobias Speckbacher, Todor Mihaylov, Tong Xiao, Ujjwal Karn, Vedanuj Goswami, Vibhor Gupta, Vignesh Ramanathan, Viktor Kerkez, Vincent Gouget, Virginie Do, Vish Vogeti, Vitor Albiero, Vladan Petrovic, Weiwei Chu, Wenhan Xiong, Wenyin Fu, Whitney Meers, Xavier Martinet, Xiaodong Wang, Xiaofang Wang, Xiaoqing Ellen Tan, Xide Xia, Xinfeng Xie, Xuchao Jia, Xuewei Wang, Yaelle Goldschlag, Yashesh Gaur, Yasmine Babaei, Yi Wen, Yiwon Song, Yuchen Zhang, Yue Li, Yuning Mao, Zacharie Delpierre Coudert, Zheng Yan, Zhengxing Chen, Zoe Papanikos, Aaditya Singh, Aayushi Srivastava, Abha Jain, Adam Kelsey, Adam Shajnfeld, Adithya Gangidi, Adolfo Victoria, Ahuva Goldstand, Ajay Menon, Ajay Sharma, Alex Boesenberg, Alexei Baevski, Allie Feinstein, Amanda Kallet, Amit Sangani, Amos Teo, Anam Yunus, Andrei Lupu, Andres Alvarado, Andrew Caples, Andrew Gu, Andrew Ho, Andrew Poulton, Andrew Ryan, Ankit Ramchandani, Annie Dong, Annie Franco, Anuj Goyal, Aparajita Saraf, Arkabandhu Chowdhury, Ashley Gabriel, Ashwin Barambe, Assaf Eisenman, Azadeh Yazdan, Beau James, Ben Maurer, Benjamin Leonhardi, Bernie Huang, Beth Loyd, Beto De Paola, Bhargavi Paranjape, Bing Liu, Bo Wu, Boyu Ni, Braden Hancock, Bram Wasti, Brandon Spence, Brani Stojkovic, Brian Gamido, Britt Montalvo, Carl Parker, Carly Burton, Catalina Mejia, Ce Liu, Changhan Wang, Changkyu Kim, Chao Zhou, Chester Hu, Ching-Hsiang Chu, Chris Cai, Chris Tindal, Christoph Feichtenhofer, Cynthia Gao, Damon Civin, Dana Beaty, Daniel Kreymeyer, Daniel Li, David Adkins, David Xu, Davide Testuggine, Delia David, Devi Parikh, Diana Liskovich, Didem Foss, Dingkan Wang, Duc Le, Dustin Holland, Edward Dowling, Eissa Jamil, Elaine Montgomery, Eleonora Presani, Emily Hahn, Emily Wood, Eric-Tuan Le, Erik Brinkman, Esteban Arcaute, Evan Dunbar, Evan Smothers, Fei Sun, Felix Kreuk, Feng Tian, Filippos Kokkinos, Firat Ozgenel, Francesco Cagioni, Frank Kanayet, Frank Seide, Gabriela Medina Florez, Gabriella Schwarz, Gada Badeer, Georgia Swee, Gil Halpern, Grant Herman, Grigory Sizov, Guangyi Zhang, Guna Lakshminarayanan, Hakan Inan, Hamid Shojanazeri, Han Zou, Hannah Wang, Hanwen Zha, Haroun Habeeb, Harrison Rudolph, Helen Suk, Henry Aspegren, Hunter Goldman, Hongyuan Zhan, Ibrahim Damlaj, Igor Molybog, Igor Tufanov, Ilias Leontiadis, Irima-Elena Veliche, Itai Gat, Jake Weissman, James Geboski, James Kohli, Janice Lam, Japhet Asher, Jean-Baptiste Gaya, Jeff Marcus, Jeff Tang, Jennifer Chan, Jenny Zhen, Jeremy Reizenstein, Jeremy Teboul, Jessica Zhong, Jian Jin, Jingyi Yang, Joe Cummings, Jon Carvill, Jon Shepard, Jonathan McPhie, Jonathan Torres, Josh Ginsburg, Junjie Wang, Kai Wu, Kam Hou U, Karan Saxena, Kartikay Khandelwal, Katayoun Zand, Kathy Matosich, Kaushik Veeraraghavan, Kelly Michelen, Keqian Li, Kiran Jagadeesh, Kun Huang, Kunal Chawla, Kyle Huang, Lailin Chen, Lakshya Garg, Lavender A, Leandro Silva, Lee Bell, Lei Zhang, Liangpeng Guo, Licheng Yu, Liron Moshkovich, Luca Wehrstedt, Madian Khabza, Manav Avalani, Manish Bhatt, Martynas Mankus, Matan Hasson, Matthew Lennie, Matthias Reso, Maxim Groshev, Maxim Naumov, Maya Lathi, Meghan Kenally, Miao Liu, Michael L. Seltzer, Michal Valko, Michelle Restrepo, Mihir Patel, Mik Vyatskov, Mikayel Samvelyan, Mike Clark, Mike Macey, Mike Wang, Miquel Jubert Hermoso, Mo Metanat, Mohammad Rastegari, Munish Bansal, Nandhini Santhanam, Natascha Parks, Natasha White, Navyata Bawa, Nayan Singhal, Nick Egebo, Nicolas Usunier, Nikhil Mehta, Nikolay Pavlovich Laptev, Ning Dong, Norman Cheng, Oleg Chernoguz, Olivia Hart, Omkar Salpekar, Ozlem Kalinli, Parkin Kent, Parth Parekh, Paul Saab, Pavan Balaji, Pedro Rittner, Philip Bontrager, Pierre Roux, Piotr Dollar, Polina Zvyagina, Prashant Ratanchandani, Pritish Vuvraj, Qian Liang, Rachad Alao, Rachel Rodriguez, Rafi Ayub, Raghotham Murthy, Raghu Nayani, Rahul Mitra, Rangrabhu Parthasarathy, Raymond Li, Rebekkah Hogan, Robin Battey, Rocky Wang, Russ Howes, Rutu Rinott, Sachin Mehta, Sachin Sibi, Sai Jayesh Bondu, Samyak Datta, Sara Chugh, Sara Hunt, Sargun Dhillon, Sasha Sidorov, Satadru Pan, Saurabh Mahajan, Saurabh Verma, Seiji Yamamoto, Sharadh Ramaswamy, Shaun Lindsay, Shaun Lindsay, Sheng Feng, Shenghao Lin, Shengxin Cindy Zha, Shishir Patil, Shiva Shankar, Shuang Zhang, Shuang Zhang, Sinong Wang, Sneha Agarwal, Soji Sajuyigbe, Soumith Chintala, Stephanie Max, Stephen Chen, Steve Kehoe, Steve Satterfield, Sudarshan Govindaprasad, Smit Gupta, Summer Deng, Sungmin Cho, Sunny Virk, Suraj Subramanian, Suy Choudhury, Sydney Goldman, Tal Remez, Tamar Glaser, Tamara Best, Thilo Koehler, Thomas Robinson, Tianhe Li, Tianjun Zhang, Tim Matthews, Timothy Chou, Tzook Shaked, Varun Vontimitta, Victoria Ajayi, Victoria Montanez, Vijai Mohan, Vinay Satish Kumar, Vishal Mangla, Vlad Ionescu, Vlad Poenaru, Vlad Tiberiu Mihalescu, Vladimir Ivanov, Wei Li, Wenchen Wang, Wenwen Jiang, Wes Bouaziz, Will Constable, Xiaocheng Tang, Xiaojian Wu, Xiaolan Wang, Xilun Wu, Xinbo Gao, Yaniv Kleinman, Yanjun Chen, Ye Hu, Ye Jia, Ye Qi, Yenda Li, Yilin Zhang, Ying Zhang, Yossi Adi, Youngjin Nam, Yu, Wang, Yu Zhao, Yuchen Hao, Yundi Qian, Yunlu Li, Yuzi He, Zach Rait, Zachary DeVito, Zef Rosnbrick, Zhaoduo Wen, Zhenyu Yang, Zhiwei Zhao, and Zhiyu Ma. 2024. The Llama 3 Herd of Models. arXiv:2407.21783 [cs.AI] <https://arxiv.org/abs/2407.21783>
- [10] Ozgur Guldogan, Jackson Kunde, Kangwook Lee, and Ramtin Pedarsani. 2024. Multi-Bin Batching for Increasing LLM Inference Throughput. arXiv:2412.04504 [cs.CL] <https://arxiv.org/abs/2412.04504>
- [11] W Keith Hastings. 1970. Monte Carlo sampling methods using Markov chains and their applications. (1970).
- [12] Woosuk Kwon, Zhuohan Li, Siyuan Zhuang, Ying Sheng, Lianmin Zheng, Cody Hao Yu, Joseph E. Gonzalez, Hao Zhang, and Ion Stoica. 2023. Efficient Memory Management for Large Language Model Serving with PagedAttention. arXiv:2309.06180 [cs.LG] <https://arxiv.org/abs/2309.06180>
- [13] Hunter Lightman, Vineet Kosaraju, Yura Burda, Harri Edwards, Bowen Baker, Teddy Lee, Jan Leike, John Schulman, Ilya Sutskever, and Karl Cobbe. 2023. Let's Verify Step by Step. arXiv:2305.20050 [cs.LG] <https://arxiv.org/abs/2305.20050>
- [14] Nicholas Metropolis and Stanislaw Ulam. 1949. The monte carlo method. *Journal of the American statistical association* 44, 247 (1949), 335–341.
- [15] Long Ouyang, Jeffrey Wu, Xu Jiang, Diogo Almeida, Carroll Wainwright, Pamela Mishkin, Chong Zhang, Sandhini Agarwal, Katarina Slama, Alex Ray, et al. 2022. Training language models to follow instructions with human feedback. *Advances in neural information processing systems* 35 (2022), 27730–27744.
- [16] Long Ouyang, Jeff Wu, Xu Jiang, Diogo Almeida, Carroll L. Wainwright, Pamela Mishkin, Chong Zhang, Sandhini Agarwal, Katarina Slama, Alex Ray, John Schulman, Jacob Hilton, Fraser Kelton, Luke Miller, Maddie Simens, Amanda Askell, Peter Welinder, Paul Christiano, Jan Leike, and Ryan Lowe. 2022. Training language models to follow instructions with human feedback. arXiv:2203.02155 [cs.CL] <https://arxiv.org/abs/2203.02155>
- [17] Reiner Pope, Sholto Douglas, Aakanksha Chowdhery, Jacob Devlin, James Bradbury, Anselm Levskaya, Jonathan Heek, Kefan Xiao, Shivani Agrawal, and Jeff Dean. 2022. Efficiently Scaling Transformer Inference. arXiv:2211.05102 [cs.LG] <https://arxiv.org/abs/2211.05102>
- [18] Haoran Qiu, Weichao Mao, Archit Patke, Shengkun Cui, Saurabh Jha, Chen Wang, Hubertus Franke, Zbigniew T. Kalbarczyk, Tamer Başar, and Ravishankar K. Iyer. 2024. Efficient Interactive LLM Serving with Proxy Model-based Sequence Length Prediction. arXiv:2404.08509 [cs.DC] <https://arxiv.org/abs/2404.08509>
- [19] Alec Radford, Jeffrey Wu, Rewon Child, David Luan, Dario Amodei, Ilya Sutskever, et al. 2019. Language models are unsupervised multitask learners. *OpenAI blog* 1, 8 (2019), 9.
- [20] Rafael Rafailov, Archit Sharma, Eric Mitchell, Stefano Ermon, Christopher D. Manning, and Chelsea Finn. 2024. Direct Preference Optimization: Your Language Model is Secretly a Reward Model. arXiv:2305.18290 [cs.LG] <https://arxiv.org/abs/2305.18290>
- [21] Samyam Rajbhandari, Jeff Rasley, Olatunji Ruwase, and Yuxiong He. 2020. ZeRO: Memory Optimizations Toward Training Trillion Parameter Models. arXiv:1910.02054 [cs.LG] <https://arxiv.org/abs/1910.02054>
- [22] Samyam Rajbhandari, Olatunji Ruwase, Jeff Rasley, Shaden Smith, and Yuxiong He. 2021. ZeRO-Infinity: Breaking the GPU Memory Wall for Extreme Scale Deep Learning. arXiv:2104.07857 [cs.DC] <https://arxiv.org/abs/2104.07857>
- [23] John Schulman, Philipp Moritz, Sergey Levine, Michael Jordan, and Pieter Abbeel. 2018. High-Dimensional Continuous Control Using Generalized Advantage Estimation. arXiv:1506.02438 [cs.LG] <https://arxiv.org/abs/1506.02438>
- [24] John Schulman, Filip Wolski, Prafulla Dhariwal, Alec Radford, and Oleg Klimov. 2017. Proximal policy optimization algorithms. *arXiv preprint arXiv:1707.06347* (2017).
- [25] Zhihong Shao, Peiyi Wang, Qihao Zhu, Runxin Xu, Junxiao Song, Xiao Bi, Haowei Zhang, Mingchuan Zhang, Y. K. Li, Y. Wu, and Daya Guo. 2024. DeepSeek-Math: Pushing the Limits of Mathematical Reasoning in Open Language Models. arXiv:2402.03300 [cs.CL] <https://arxiv.org/abs/2402.03300>
- [26] Guangming Sheng, Chi Zhang, Zilingfeng Ye, Xibin Wu, Wang Zhang, Ru Zhang, Yanghua Peng, Haibin Lin, and Chuan Wu. 2025. Hybridflow: A flexible and efficient rlhf framework. In *Proceedings of the Twentieth European Conference on Computer Systems*. 1279–1297.
- [27] Luohe Shi, Hongyi Zhang, Yao Yao, Zuchao Li, and Hai Zhao. 2024. Keep the Cost Down: A Review on Methods to Optimize LLM's KV-Cache Consumption. arXiv:2407.18003 [cs.CL] <https://arxiv.org/abs/2407.18003>
- [28] Hugo Touvron, Thibaut Lavril, Gautier Izacard, Xavier Martinet, Marie-Anne Lachaux, Thimothée Lacroix, Baptiste Rozière, Naman Goyal, Eric Hambro,

Faisal Azhar, Aurelien Rodriguez, Armand Joulin, Edouard Grave, and Guillaume Lample. 2023. LLaMA: Open and Efficient Foundation Language Models. arXiv:2302.13971 [cs.CL] <https://arxiv.org/abs/2302.13971>

[29] Hugo Touvron, Louis Martin, Kevin Stone, Peter Albert, Amjad Almahairi, Yasmine Babaei, Nikolay Bashlykov, Soumya Batra, Prajwal Bhargava, Shruti Bhosale, Dan Bikel, Lukas Blecher, Cristian Canton Ferrer, Moya Chen, Guillem Cucurull, David Esiobu, Jude Fernandes, Jeremy Fu, Wenyin Fu, Brian Fuller, Cynthia Gao, Vedanuj Goswami, Naman Goyal, Anthony Hartshorn, Saghar Hosseini, Rui Hou, Hakan Inan, Marcin Kardas, Viktor Kerkez, Madian Khabsa, Isabel Kloumann, Artem Korenev, Punit Singh Koura, Marie-Anne Lachaux, Thibaut Lavril, Jenya Lee, Diana Liskovich, Yinghai Lu, Yuning Mao, Xavier Martinet, Todor Mihaylov, Pushkar Mishra, Igor Molybog, Yixin Nie, Andrew Poulton, Jeremy Reizenstein, Rashi Rungta, Kalyan Saladi, Alan Schelten, Ruan Silva, Eric Michael Smith, Ranjan Subramanian, Xiaoqing Ellen Tan, Binh Tang, Ross Taylor, Adina Williams, Jian Xiang Kuan, Puxin Xu, Zheng Yan, Iliyan Zarov, Yuchen Zhang, Angela Fan, Melanie Kambadur, Sharan Narang, Aurelien Rodriguez, Robert Stojnic, Sergey Edunov, and Thomas Scialom. 2023. Llama 2: Open Foundation and Fine-Tuned Chat Models. arXiv:2307.09288 [cs.CL] <https://arxiv.org/abs/2307.09288>

[30] Chulin Xie, Yangsibo Huang, Chiyuan Zhang, Da Yu, Xinyun Chen, Bill Yuchen Lin, Bo Li, Badih Ghazi, and Ravi Kumar. 2025. On Memorization of Large Language Models in Logical Reasoning. arXiv:2410.23123 [cs.CL] <https://arxiv.org/abs/2410.23123>

[31] An Yang, Anfeng Li, Baosong Yang, Beichen Zhang, Binyuan Hui, Bo Zheng, Bowen Yu, Chang Gao, Chengen Huang, Chenxu Lv, Chujie Zheng, Dayiheng Liu, Fan Zhou, Fei Huang, Feng Hu, Hao Ge, Haoran Wei, Huan Lin, Jialong Tang, Jian Yang, Jianhong Tu, Jianwei Zhang, Jianxin Yang, Jiayi Yang, Jing Zhou, Jingren Zhou, Junyang Lin, Kai Dang, Keqin Bao, Kexin Yang, Le Yu, Lianghao Deng, Mei Li, Mingfeng Xue, Mingze Li, Pei Zhang, Peng Wang, Qin Zhu, Rui Men, Ruize Gao, Shixuan Liu, Shuang Luo, Tianhao Li, Tianyi Tang, Wenbiao Yin, Xingzhang Ren, Xinyu Wang, Xinyu Zhang, Xuancheng Ren, Yang Fan, Yang Su, Yichang Zhang, Yinger Zhang, Yu Wan, Yuqiong Liu, Zekun Wang, Zeyu Cui, Zhenru Zhang, Zhipeng Zhou, and Zihan Qiu. 2025. Qwen3 Technical Report. arXiv:2505.09388 [cs.CL] <https://arxiv.org/abs/2505.09388>

[32] Lianmin Zheng, Wei-Lin Chiang, Ying Sheng, Tianle Li, Siyuan Zhuang, Zhanghao Wu, Yonghao Zhuang, Zhuohan Li, Zi Lin, Eric P Xing, Joseph E. Gonzalez, Ion Stoica, and Hao Zhang. 2023. LMSYS-Chat-1M: A Large-Scale Real-World LLM Conversation Dataset. arXiv:2309.11998 [cs.CL]

[33] Lianmin Zheng, Liangsheng Yin, Zhiqiang Xie, Chuyue Sun, Jeff Huang, Cody Hao Yu, Shiyi Cao, Christos Kozyrakis, Ion Stoica, Joseph E. Gonzalez, Clark Barrett, and Ying Sheng. 2024. SGLang: Efficient Execution of Structured Language Model Programs. arXiv:2312.07104 [cs.AI] <https://arxiv.org/abs/2312.07104>

[34] Zhen Zheng, Xin Ji, Taosong Fang, Fanghao Zhou, Chuanjie Liu, and Gang Peng. 2025. BatchLLM: Optimizing Large Batched LLM Inference with Global Prefix Sharing and Throughput-oriented Token Batching. arXiv:2412.03594 [cs.CL] <https://arxiv.org/abs/2412.03594>

[35] Yinmin Zhong, Zili Zhang, Xiaoniu Song, Hanpeng Hu, Chao Jin, Bingyang Wu, Nuo Chen, Yukun Chen, Yu Zhou, Changyi Wan, et al. 2025. StreamRL: Scalable, Heterogeneous, and Elastic RL for LLMs with Disaggregated Stream Generation. arXiv preprint arXiv:2504.15930 (2025).

Appendix

A More Figures

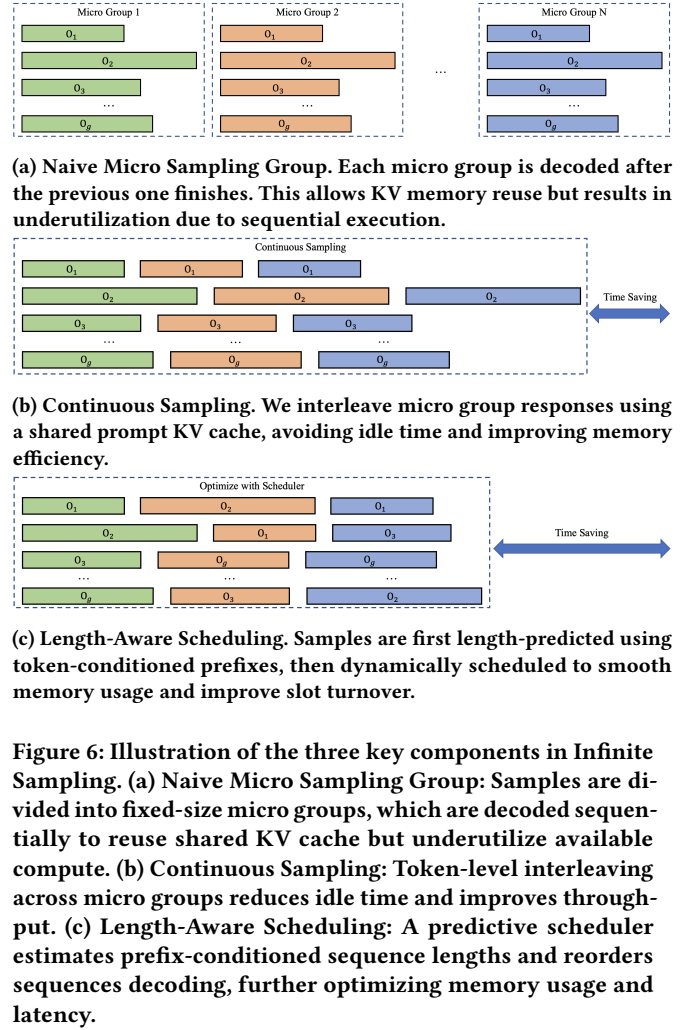


Figure 6: Illustration of the three key components in Infinite Sampling. (a) **Naive Micro Sampling Group:** Samples are divided into fixed-size micro groups, which are decoded sequentially to reuse shared KV cache but underutilize available compute. (b) **Continuous Sampling:** Token-level interleaving across micro groups reduces idle time and improves throughput. (c) **Length-Aware Scheduling:** A predictive scheduler estimates prefix-conditioned sequence lengths and reorders sequences decoding, further optimizing memory usage and latency.

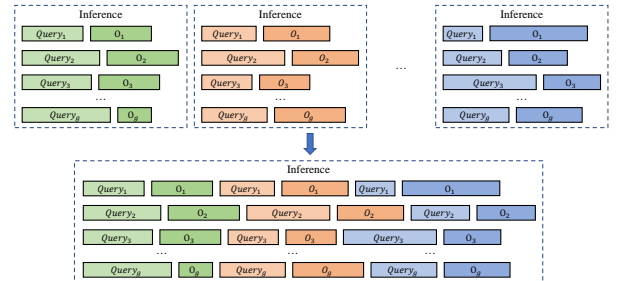


Figure 7: Continuous Batching in inference merges unrelated prompts and responses to eliminate bubbles. Not directly usable in GRPO.